Robert B. Sparkes | Niels Hovius | Albert Galy | James T. Liu

Survival of graphitized petrogenic organic carbon through multiple erosional cycles

Suggested citation referring to the original publication:
Earth and Planetary Science Letters 531 (2020) 115992
DOI https://doi.org/10.1016/j.epsl.2019.115992
ISSN 1385-013X (online), 0012-821X (print)

Earth and Planetary Science Letters 531 (2020) 115992

Contents lists available at ScienceDirect

Earth and Planetary Science Letters

www.elsevier.com/locate/epsl

Survival of graphitized petrogenic organic carbon through multiple erosional cycles

Robert B. Sparkes [a,b,*], Niels Hovius [c], Albert Galy [d], James T. Liu [e]

[a] Ecology and Environment Research Centre, Department of Natural Sciences, Manchester Metropolitan University, Manchester, UK
[b] Department of Materials Science and Metallurgy, University of Cambridge, Cambridge, UK
[c] GFZ German Research Centre for Geosciences, Telegrafenberg, 14473 Potsdam, Germany
[d] CRPG - CNRS - Université de Lorraine BP20, 54501 Vandœuvre-lès-Nancy, France
[e] Department of Oceanography, National Sun Yat-sen University, Kaohsiung, Taiwan

ARTICLE INFO

Article history:
Received 31 March 2018
Received in revised form 17 October 2019
Accepted 27 November 2019
Available online 9 December 2019
Editor: L. Derry

Keywords:
graphite
organic carbon
orogeny
recycling
Raman spectroscopy
erosion

ABSTRACT

Graphite forms the endpoint for organic carbon metamorphism; it is extremely resilient to physical, biological and chemical degradation. Carbonaceous materials (CM) contained within sediments, collected across Taiwan and from the Gaoping submarine canyon, were analyzed using Raman spectroscopy to determine the crystallinity. This allowed the erosional and orogenic movements of petrogenic organic carbon (OC_{petro}) during the Taiwanese orogeny to be deduced. After automatically fitting and classifying spectra, the distribution of four groups of CM within the sediments provides evidence that many forms of OC_{petro} have survived at least one previous cycle of erosion, transport and burial before forming rocks in the Western Foothills of the island. There is extensive detrital graphite present in rocks that have not experienced high-grade metamorphism, and graphite flakes are also found in recently deposited marine sediments off Taiwan. The tectonic and geological history of the island shows that these graphite flakes must have survived at least three episodes of recycling. Therefore, transformation to graphite during burial and orogeny is a mechanism for stabilizing organic carbon over geological time, removing biospheric carbon from the active carbon cycle and protecting it from oxidation during future erosion events.

1. Introduction

Erosion drives the transfer of Particulate Organic Carbon (POC) to geological basins, where its long-term preservation is helped by rapid burial and/or anoxic conditions (France-Lanord and Derry, 1997; Galy et al., 2007; Hilton et al., 2015; Walsh et al., 1981). This is a key feature of the global carbon cycle, syphoning large amounts of atmospheric carbon into the lithosphere. Erosion also exposes previously buried petrogenic carbon (OC_{petro}) at the Earth's surface, promoting the release of CO_2 via microbial or chemical degradation (Hemingway et al., 2018; Petsch et al., 2000). For the organic pathway to carbon sequestration to be effective on geological time scales, a net transfer has to occur from the atmosphere-surface system into geological storage. Although this transfer appears to be efficient in mountain belts where short, steep transport lines connect source and sink (Galy et al., 2007; Hilton et al., 2008; Kao et al., 2014), these settings are prone to rapid tectonic recycling, and carbon may reflux into the atmosphere, especially if the OC_{petro} is biologically-available or prone to physical decay. Graphitization by deep burial renders carbon more recalcitrant, which may limit losses during orogenic recycling (e.g. Galy et al., 2008). Survival rates of OC_{petro} during single cycles of erosion and deposition have been estimated at between 15% and 85%, with shorter distances between source and sink leading to better preservation (Galy et al., 2008; Hilton et al., 2008; Bouchez et al., 2010). With high survival rates, the ability for OC_{petro} to persist over multiple cycles of burial and exhumation is possible, but has not been demonstrated. Here, we address this knowledge gap, showing that in the rapidly exhuming mountains of Taiwan, highly graphitized OC_{petro} can escape degradation during repeated erosional cycles. This raises the prospect of progressive accumulation of POC in geological basins, provided that tectonic burial is sufficiently deep to drive graphitization.

* Corresponding author at: Ecology and Environment Research Centre, Department of Natural Sciences, Manchester Metropolitan University, Manchester, UK.
E-mail address: robert.sparkes@cantab.net (R.B. Sparkes).

https://doi.org/10.1016/j.epsl.2019.115992

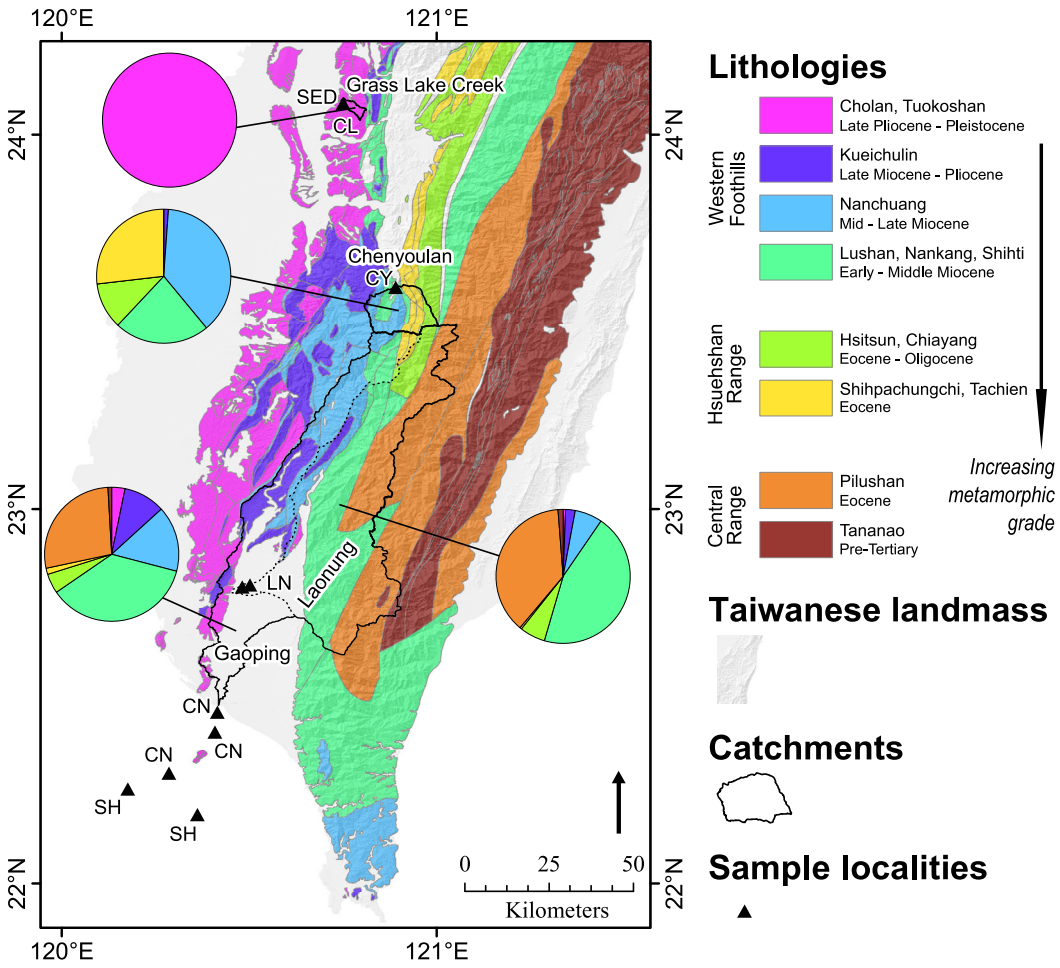

Fig. 1. Geological map of southern Taiwan, showing catchments sampled in this study. Major stratigraphic groups are shown, along with representative formations and their ages. Sample sites are shown by black triangles. SH: Gaoping Shelf, CN: Gaoping Submarine Canyon, LN: Laonung River, CY: Chenyoulan River, SED: Grass Lake Creek sediment, CL: Grass Lake Creek coal.

2. Geological and tectonic setting

Mountain building in Taiwan is associated with the rapid and ongoing convergence of the Philippine Sea plate and the Asian continental margin (Teng, 1990). Until 3 Ma, the Taiwan segment of the Asian margin experienced passive margin sedimentation, dominated by fine-grained clastic input. Since then, continental margin deposits and underlying marine sediments of Miocene-Pleistocene age have accreted along the western mountain front, and progressively uplifted to form the Western Foothills fold and thrust belt. These rocks have undergone little metamorphism (Yui and Chu, 2000). In the central and northern part of the island, they abut the Hsuehshan Range, which consists of an Eocene-Oligocene passive margin sedimentary sequence, metamorphosed during the Plio-Pleistocene from prehnite-pumpellyite facies up to greenschist facies (Chen et al., 1983, 2019; Yui and Chu, 2000). Further south and east, the Central Range consists of Tertiary and older metasedimentary rocks that have also experienced this range of metamorphic conditions, and up to amphibolite facies in the Tananao Complex, which includes carbon-rich black schists. Major formations and stratigraphic groups are shown in Fig. 1.

The emergent mountain belt has been shedding sediment to the west, into the shallow sea between Taiwan and the Asian mainland. In this basin, a transition from Chinese continental to Taiwanese orogenic sediment sources occurred in the early-mid Pliocene (Teng, 1990). While older Taiwan-derived sediments are all submarine, rocks of the younger Cholan and Tuokoshan formations have subaerial components, representing the precursors of the river fans that dominate the modern coastal plain of west Taiwan. The deposits of the Taiwan Strait are prone to orogenic recycling, but to the south, sediment can escape into the Manila trench, and to the north into the Okinawa backarc basin. On million-year timescales, exhumation in Taiwan is more or less balanced by erosion. Local erosion rates up to 6.0 mm y^{-1} deliver 500 Mt y^{-1} sediment to the ocean (Dadson et al., 2003). Some rocks are rapidly recycled from shallow exhumation trajectories, whilst others were brought up from deep within the orogen (Beyssac et al., 2007; Teng, 1990).

The Taiwan Central Range contains carbon-bearing metamorphic units, with up to 0.54% OC in black schists, whilst low-grade rocks in the Western Foothills contain up to 0.65% OC along with larger coal clasts (Hilton et al., 2010). Here we use Raman spectroscopy on samples collected offshore and from rivers draining the Central Range and Western Foothills to investigate recycling of OC_{petro} during the Taiwan orogeny. Raman spectroscopy of carbonaceous material (CM; material that has been partially or wholly transformed from organic matter into graphite) can be used to determine the thermal history of geological samples through the degree of OC_{petro} graphitization, which has been shown to increase systematically between 200 °C (extremely amorphous) and 645 °C (completely crystalline) (Beyssac et al., 2002a, 2003; Lahfid et al., 2010). This relationship has also been used as a sediment source marker to understand sedimentary processes (Nibourel et al., 2015; Sparkes et al., 2013, 2018). Sediment from multiple sources can be

deconvolved by characterising the distribution of different classes of OC_{petro} within a heterogeneous sample (Sparkes et al., 2018). Taiwanese lithologies have experienced a range of metamorphic conditions, and therefore host a wide distribution of OC_{petro} crystal structures (Sparkes et al., 2013). A thorough survey of Taiwanese bedrock by Beyssac et al. (2007) found that autochthonous OC_{petro} in rocks of the Central Range and Hueshuan Range bear evidence of metamorphic temperatures ranging from <330 to 516 °C, below the threshold for complete graphitization (645 °C). They also found rare graphite flakes in the Miocene formations of west Taiwan, which petrography deemed detrital.

The wide range of OC_{petro} metamorphism present in Taiwan allows individual catchments to be fingerprinted using Raman spectroscopy. Additionally, the typhoon-prone climate causes large volumes of sediment to be harvested episodically from across Taiwan and delivered to the surrounding seas via hyperpycnal flows, where an integrated sedimentary signal can be recovered from offshore samples. One such episode followed typhoon Morakot in August 2009. This typhoon generated significant deposition of terrestrial sediment in the Gaoping submarine canyon and Manila trench (Sparkes et al., 2015; Carter et al., 2014). Radiocarbon dating showed that the organic matter in these sediments was dominated by OC_{petro}, with a fraction modern organic carbon of 0.34 (Sparkes et al., 2015).

3. Materials and methods

3.1. Sample sites

This study is focused on the closely coupled Gaoping River and Canyon system (Liu et al., 2016). The Gaoping River is the second largest in Taiwan, with a drainage area of 3257 km^2, and an average annual sediment load of about 50 $Mt\,y^{-1}$ (Dadson et al., 2003). Within this watershed are rocks from a wide range of lithological groups. The Laonung tributary drains 63% of the catchment (see Fig. 1). This fraction comprises predominantly Eocene Central Range units, especially the Lushan and Pilushan formations, and Miocene rocks from the Western Foothills, along with some Oligocene units of the Hsueshuan Range and a minor amount of pre-Tertiary Central Range. The lower part of the Gaoping catchment drains younger Western Foothills rocks, from the Mid Miocene to Pliocene formations, and a small amount of Eocene Hsuehshan Range material. Erosion rates vary across the study area, and are highest where high storm frequency coincides with weak substrates and rapid tectonic deformation (Dadson et al., 2003). Therefore the younger, less metamorphosed lithologies within the Gaoping and Laonung catchments are likely to contribute relatively more sediment to the fluvial and marine system.

Sediments (sample code “LN”), with coarse sand to silt-sized grains, were collected from a river bar and flood deposits on the banks of the Laonung River after typhoon Morakot (see Sparkes et al., 2015, and the supporting information for further details).

To better characterize the variety of formations within the Gaoping catchment, two smaller catchments draining a restricted range of outcropping formations were sampled further north in Taiwan (Fig. 1). First, the Chenyoulan River in central Taiwan drains rocks of Eocene to Miocene age from the Hsueshuan Range and Western Foothills but, in contrast to the Laonung River, does not comprise formations belonging to the Central Range. Suspended sediment samples were collected from the Chenyoulan River (“CY”) before typhoon Fanapi (2010) and on the rising limb of the typhoon flood. Second, the Grass Lake Creek in Taichung County drains exclusively Plio-Pleistocene age material from the Western Foothills’ Cholan and Tuokoshan Formations (Chen et al., 2001). Hand specimens of sandstone from the river bedload (“SED”) represent material from across the catchment. In addition, cm-sized lignite-grade coal (“CL”) was recovered from the bedload, which can be used to determine the metamorphic/diagenetic grade attained by organic matter within these formations after deposition (Beyssac et al., 2002a; Lahfid et al., 2010; Sparkes et al., 2013).

The Gaoping River connects to the Gaoping Canyon, immediately offshore. The canyon is a sinuous erosive feature within the 45 km wide continental shelf, through which material is transferred to the deep ocean basin of the South China Sea. During and after typhoon Morakot, turbidity currents, which are frequently observed following storm events in Taiwan (Liu et al., 2012, 2013), transported sediment to long-term storage in the Manila Trench, hundreds of kilometres from the sediment source (Carter et al., 2014). Samples were collected by box coring of canyon (“CN”) and shelf (“SH”) sediments following the typhoon (cruise OR1-915). These samples are dominated by terrestrial sediment, especially in the canyon but also the core-top of the shelf sediments (Sparkes et al., 2015). Based on elemental and isotopic characterisation, the major component of their organic carbon load was OC_{petro}, likely from the Laonung River (Sparkes et al., 2015).

Fig. 1 shows the proportion of each lithology group in the catchments above each sample location. Proportions were calculated based on the 2D area fraction of a digital geological map situated within each catchment (Chen et al., 2000). Multiple lithologies were grouped together to form the larger units, see Fig. 1 for the groupings. Further sampling details, and lithological area calculation results, are in the supporting information.

3.2. Raman spectroscopy

The physical changes that occur during graphitization could significantly increase the resilience of OC_{petro} during erosion and transport. Raman spectroscopy has been used to interrogate the crystal structure of OC_{petro} within rocks and sediments ((e.g. Beyssac et al., 2002b, 2003, 2007; Nibourel et al., 2015; Sparkes et al., 2013). Spectra were collected from ground and homogenized powders, analyzed using automated routines and classified into four groups using peak area and width parameters (Sparkes et al., 2013, see Fig. 2 for example spectra; see the supporting information for full method details). These groups are Disordered, Intermediate Grade, Mildly Graphitized, and Highly Graphitized OC_{petro}.

4. Results

194 spectra were collected from 19 samples. Each spectrum was classified using the spectral parameters described above, and the results are shown per catchment group in Fig. 3. These spectra cover a wide range, from extremely disordered OC_{petro} to perfectly crystalline graphite. With heterogeneous mixtures like these, it is difficult to collect enough Raman spectra for full quantitative analysis of each spectral group. Moreover, total OC concentrations in our sample materials are relatively low, meaning that the number of spectra collected per sample do not allow statistical treatment of the dataset. Therefore, we are restricted to documenting the presence or absence of each spectral group. There are OC_{petro} classes that are notably present or absent in samples from particular locations.

The Gaoping Canyon (CN) and Shelf (SH) contain all four classes of OC_{petro}, particularly the Intermediate Grade. Mildly and Highly graphitized OC_{petro} are present in both of these sample groups. Onshore, the Laonung River (LN) contains mostly Intermediate Grade OC_{petro}, with one spectrum classed as Mildly Graphitized. The Chenyoulan River (CY) samples also contained mostly Intermediate

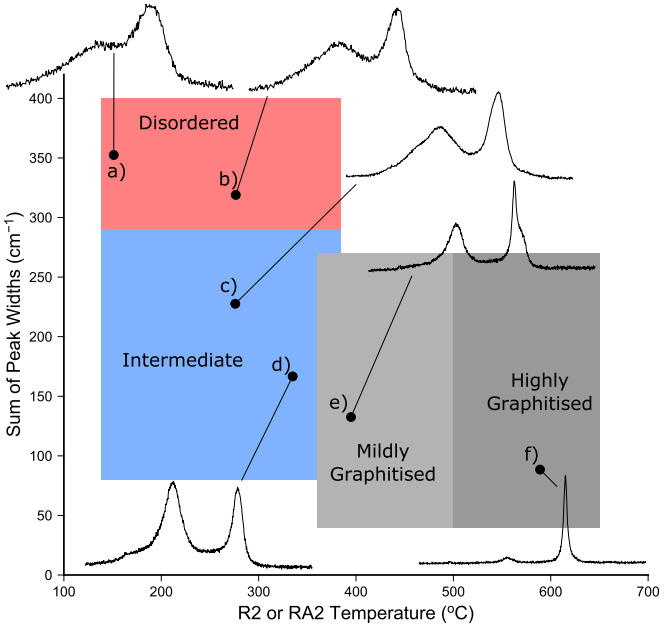

Fig. 2. Examples of Raman spectra from a range of OC_{petro} analyzed in a single sedimentary sample. Sum of peak widths (G + D1 + D2) is plotted against metamorphic temperature (Beyssac et al., 2002a; Lahfid et al., 2010). Spectral classes used in this study are labelled and shown using coloured boxes (red = Disordered, blue = Intermediate Grade, light grey Mildly Graphitized, dark grey = Highly graphitized) Spectra a) through to f) demonstrate a reduction in peak width and an increase in inferred temperature, denoting an increase in crystallinity during the transition from amorphous carbon into graphite.

Grade OC_{petro}, with some Mildly Graphitized OC_{petro} (at the Intermediate Grade end of this class) and minor amounts of Disordered OC_{petro}. The Grass Lake Creek sediment (SED) contained all four classes of spectra, but the two extreme categories (Highly Graphitized and Disordered OC_{petro}) are more abundant. The coal clast (CL) collected from Grass Lake Creek produced only spectra in the Disordered class, with extremely wide Raman peaks and very little inter-spectra variation.

5. Discussion

The collected Raman spectra, combined with geological maps and tectonic, sedimentary and fluvial information about Taiwan and China, allow us to attempt the following: identify the likely source litholog(ies) for each class of Raman spectra; track the movement of OC_{petro} through one or more erosion - burial - exhumation cycles; propose a source of Highly Graphitized OC_{petro} found in Taiwanese sediments, and infer the consequences for the carbon cycle of graphite exhumation and erosion.

5.1. Source lithologies of different OC_{petro} types

Combining geological maps with Raman data allows the source lithologies of each OC_{petro} class to be inferred.

5.1.1. Source of highly graphtized OC_{petro}

The Central Range, Hsuehshan Range and Early-Mid Miocene Western Foothills contain formations with highest metamorphic grade in the study area, making up the major proportion of the Laonung (LN samples) and Chenyoulan (CY samples) river catchments (Figs. 1 and 4). OC_{petro} with the highest degree of crystallinity would be expected to come from these formations, and be seen in samples LN and CY. However, Highly Graphitized OC_{petro} was not found in these samples. Highly Graphitized OC_{petro} was only found in the Gaoping Canyon, Gaoping Shelf and the Plio-Pleistocene Grass Lake Creek sediments (CN, SH, SED; see Figs. 3 and 4). Formations younger than the Mid Miocene forms only 3% of the Laonung catchment area, but 41% of the remainder of the Gaoping River catchment. Paradoxically, the source of Highly Graphitized OC_{petro} to the Gaoping Canyon and Shelf appears to be the formations that are present exclusively in the lower Gaoping River basin, namely Mid Pliocene to Pleistocene sediments with low or no metamorphism.

5.1.2. Source of mildly graphtized and disordered OC_{petro}

This pattern repeats for Mildly Graphitized spectra, which are found in the offshore (CN, SH) and SED samples, but form only a minor component of the LN and CY samples. Similarly, Disordered grade OC_{petro} is present in the CN and SH samples, but not in the LN samples and only represents a minor component in the CY samples (see Figs. 3 and 4). SED samples are dominated by Disordered OC_{petro}, and CL is entirely Disordered (Fig. 3). This suggests that the Cholan and Tuokoshan formations, exposed in the Grass Lake Creek catchment and the lower part of the Gaoping River catchment, are the source of Disordered OC_{petro}. A large coal clast within finer sediments is highly unlikely to be detrital, so we assume that it records the maximum diagenetic conditions in the surrounding rocks, which Raman geothermometers constrain to <180 °C (Lahfid et al., 2010). The lack of Disordered OC_{petro} in the LN samples, and its paucity in CY sediments, would suggest that the Late Miocene - Pleistocene formations within the lower Gaoping River catchment are also the principal source of the Disordered OC_{petro} found offshore.

5.1.3. Source of intermediate grade OC_{petro}

Conversely, there is plentiful Intermediate Grade OC_{petro} found in the samples sourced from the more internal parts of the mountain belt (CN, SH, LN and CY), but there is relatively less of this in the SED samples (see Fig. 3). The Hsuehshan and Central range units are more metamorphosed than the Western Foothills, and are the likely source of Intermediate Grade OC_{petro} to the Gaoping Canyon (Beyssac et al., 2007; Chen et al., 1983; Yui and Chu, 2000).

Fig. 4 summarizes these findings in a Venn-style diagram. Four large overlapping circles define areas that are unique to particular catchments, or shared by two or more. Formations (coloured circles) and OC_{petro} classes (diamonds) are plotted in the area corresponding to the catchments in which they are found. The youngest, weakest, rocks of the Western Foothillls contain Highly Graphtized, Mildly Graphitized and Disordered OC_{petro}, while the more metamorphosed formations in the main mountain range contain mostly Intermediate Grade OC_{petro}. Since erosion in Taiwan is linked to lithology strength (Dadson et al., 2003), the small exposure of Western Foothills formations in the lower reaches of the Gaoping River may be contributing a large proportion of the OC_{petro} to the CN and SH samples, hence the offshore sediments deposited following Typhoon Morakot are dominated by material eroded from the floodplain, not the mountain belt.

5.2. OC_{petro} survival through an erosion - burial - exhumation cycle

Studies of the transport and erosion of OC_{petro} have shown that while disordered or semi-ordered material may be lost during long-distance fluvial transfer, crystalline graphite can survive erosion and transfer over thousands of kilometres (Bouchez et al., 2010; Galy et al., 2008; Scheingross et al., 2019). However, little is known about the resilience of OC_{petro} during sedimentary burial and subsequent tectonic and erosional exhumation. Given the presence of autochthonous Disordered OC_{petro} in the monolithological Grass Lake Creek catchment, any Intermediate Grade, Mildly Graphitized and Highly Graphitized OC_{petro} in these samples

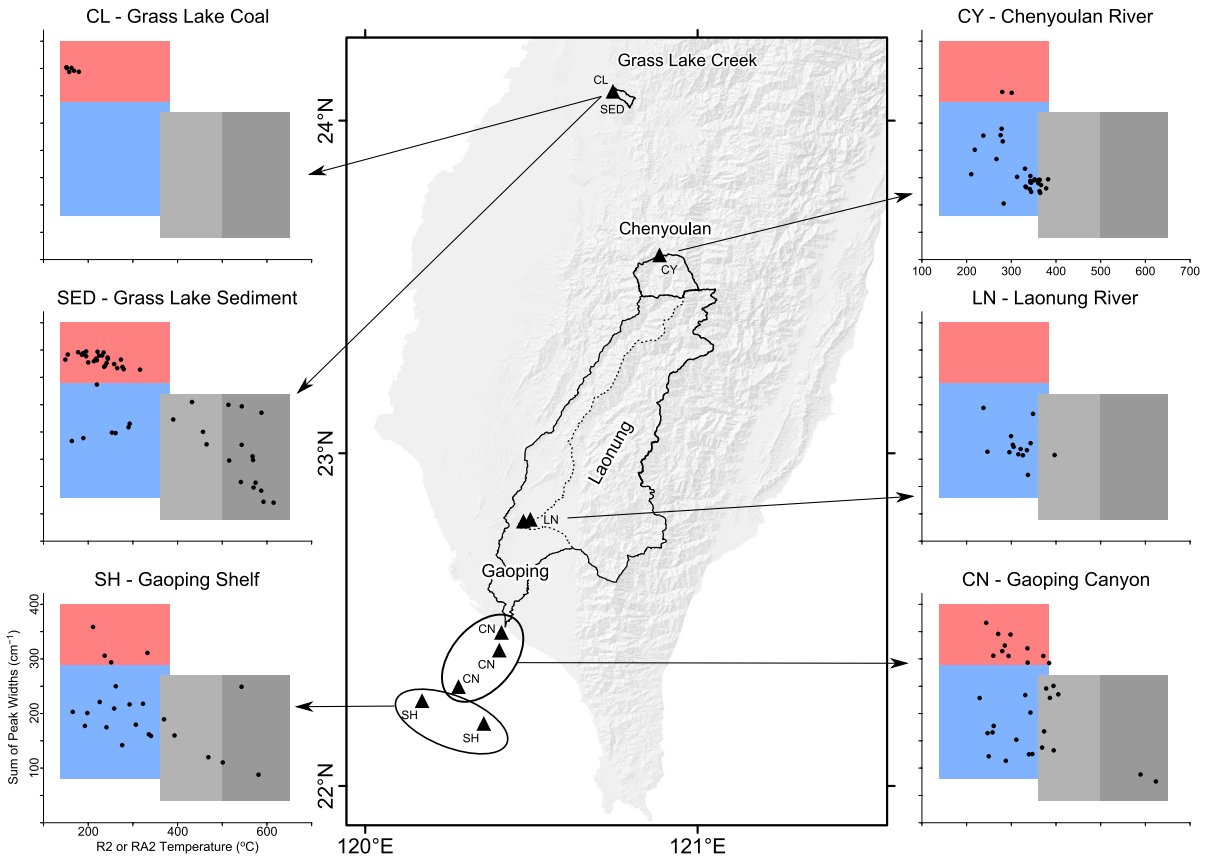

Fig. 3. Distribution of spectral properties for all samples, grouped by catchment. Sum of peak widths plotted against metamorphic temperature and classified as in Fig. 2. Presence of absence of spectra from each class was used to determine sediment provenance.

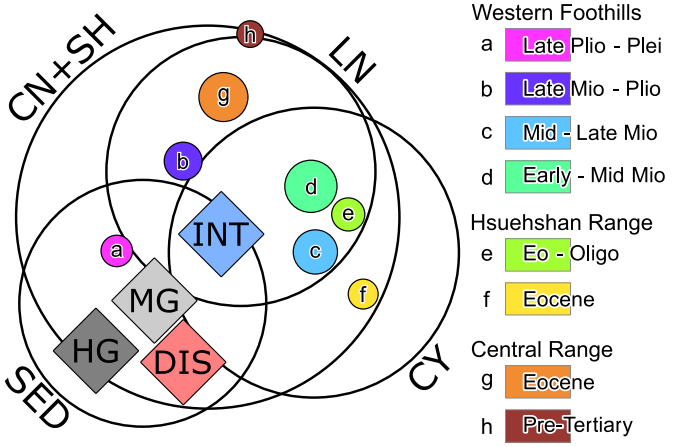

Fig. 4. Venn diagram showing which lithology groups and OC_{petro} classes are present in each catchment (CN = Gaoping Canyon, SH = Gaoping Shelf, LN = Laonung, CY = Chenyoulan, SED = Grass Lake Creek. Coloured circles (a = youngest, h = oldest) match the lithological groups identified in Fig. 1. Larger circles show lithologies that contribute a larger area to the total catchment size (all four catchments combined). Diamonds show which OC_{petro} classes are present in each catchment, colours match Figs. 2 and 3. DIS = Disordered, INT = Intermediate Grade, MG = Mildly Graphitized, HG = Highly Graphitized. Circles/diamonds overlapping the edge of a catchment shows that the lithology or OC_{petro} class is a minor contributor to that catchment.

must be detrital, transported in following formation elsewhere. OC_{petro} in these higher grade classes, therefore, has survived a longer pathway involving at the least $OC_{biosphere}$ burial, CM formation, exhumation, erosion, reburial, and re-exhumation.

5.3. OC_{petro} survival during exhumation and erosion in a large catchment

Since the Gaoping River catchment receives sediment from many formations, a range of autochthonous OC_{petro} could be sourced directly. Late Miocene - Pleistocene material of the Western Foothills outcrops in the lower reaches of the Gaoping River. Erosion from these low-grade units would deliver Disordered OC_{petro} offshore after one cycle of $OC_{biosphere}$ burial - CM formation - exhumation - erosion. Beyssac et al. (2007) measured maximum metamorphic temperatures of 516 ± 8 °C, in the Tananao Schist complex of the Pre-Tertiary Central Range, but the majority of their Hueshuan and Central Range samples produced temperatures of 350 - 450 °C, corresponding to Mildly Graphitized OC_{petro} at most (Fig. 2). Therefore erosion of these formations by the Laonung River could supply autochthonous Intermediate Grade and Mildly Graphitized OC_{petro} to the Gaoping Canyon and Shelf system from just one cycle of $OC_{biosphere}$ burial - CM formation - exhumation - erosion. Fig. 3 suggests that this could be the case, although these OC_{petro} classes are also present in SED, so erosion of Western Foothills formations by the lower branch of the Gaoping River could also supply detrital Intermediate Grade and Mildly Graphitized OC_{petro} to samples CN and SH.

However, there is no evidence of metamorphism capable of creating Highly Graphitized OC_{petro} within Taiwan (Beyssac et al., 2007; Chen et al., 1983; Yui and Chu, 2000). Therefore, the Highly graphitized OC_{petro} found in CN and SH must be detrital. We propose that it is sourced from erosion of young, weakly lithified rocks in the lower reaches of the Gaoping (e.g. Cholan and Tuokoshan formations, shown by SED to contain Highly Graphitized OC_{petro}). As in the Grass Lake Creek catchment, these particles of Highly Graphitized OC_{petro} have survived $OC_{biosphere}$ burial - graphite for-

mation - exhumation - erosion - burial - exhumation before being eroded by Typhoon Morakot.

5.4. OC_{petro} survival through multiple erosion - burial - exhumation cycles

Highly Graphitized OC_{petro} requires intense metamorphic conditions to form, and we now attempt to trace the sedimentary and tectonic history of our samples back to a plausible geological source. Highly Graphitized OC_{petro} was observed in the Plio-Pleistocene Cholan and Tuokoshan formations (SED samples), and in the Gaoping catchment samples downstream of these formations (CN and SH) but not in material from the Hueshuan and Central ranges (CY and LN). Beyssac et al. (2007) observed a few detrital graphite grains in the Tachien Sandstone (Hueshuan Range), but these were not observed in LN or CY. The Tachien Sandstone forms 14% of the Chenyoulan catchment, and <1% of the Laonung, so it is unlikely to be the source of Highly Graphitized OC_{petro} in CN and SH.

The Plio-Pleistocene formations comprise terrestrial and shallow-marine sediments sourced from the emerging Taiwan orogen (Chen et al., 2001). Careful field sampling campaigns across the core of the mountain belt have not found any autochthonous Highly Graphitized OC_{petro}, or even high concentrations of detrital graphite. Even the highest grade rocks exhumed on the island to date only contain Mildly Graphitized OC_{petro} (Beyssac et al., 2007), and it would be unusual to completely erode a high-grade metamorphic rock, leaving lower grade, stratigraphically higher, material behind. The original graphite source must therefore be external to the island. Hence, this graphite must have experienced at least two cycles of erosion - burial - exhumation prior to deposition in the Plio-Pleistocene foreland of west Taiwan. We postulate that the graphite found in the Pliocene - Pleistocene units, and by extension the Gaoping Canyon system, was originally sourced from erosion of mainland China, and deposited in a sedimentary unit that was comprehensively excavated during the emergence of Taiwan.

5.5. Long-distance transport of highly graphitized OC_{petro}

If China is the source of the graphite in Taiwanese sediments, there should be both a viable supply of eroding graphite on the mainland, and a plausible transport route. China contains the largest reserves of crystalline graphite in the world (Wilde et al., 1999). Graphite formed by contact metamorphism is present in south-eastern China, mined commercially in Hunan province (Zheng et al., 1996), drained by the Yangtze River. Detrital Highly Graphitized OC_{petro} from the Yangtze Block basement has been characterised by Raman (Ye et al., 2019). Currently the Yangtze flows into the East China Sea, where north-flowing currents take material away from Taiwan. However, the middle Yangtze region used to flow southwest into the Red River, and was only captured for eastward flow sometime between 36.5 and 23 Ma (Zheng et al., 2013). Graphite from the Red River could have been delivered to the South China Sea continental shelf until the late Eocene, or even late Oligocene, before the Yangtze changed direction. The lack of abundant detrital graphite within the Central Range units (CY and LN), suggests that graphite delivery to the China continental margin was not ubiquitous. Our proposed pathway involves a marine transport distance of around 1500 km, in addition to up to 1000 km fluvial transport. These distances are shorter than, but comparable to, those observed by Galy et al. (2007) in the Ganges-Brahmaputra system. Over such distances, up to 50% of detrital Highly Graphitized OC_{petro} can be preserved (Galy et al., 2008). If Highly Graphitized OC_{petro} is able to survive physical damage and chemical oxidation during long-range transport (Scheingross et al., 2019) then the transport across the South China Sea can take a considerable time without impacting our proposed process.

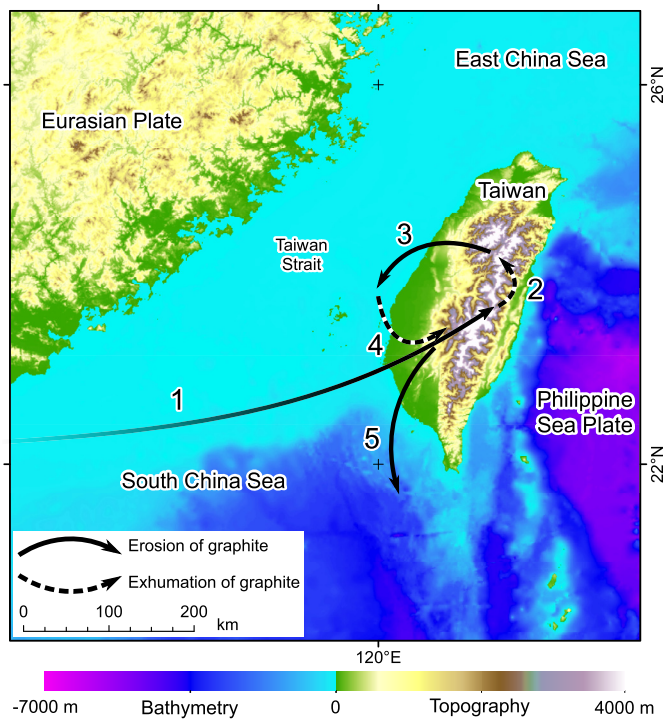

Fig. 5. The proposed path of Highly Graphitized OC_{petro}. Solid arrows represent erosional pathways, dashed arrows orogenic movements. Following erosion on mainland China, graphite was transported to the South China Sea [1], uplifted as part of the emerging Taiwan orogen [2], and recycled into Plio-Pleistocene age foreland sediments [3]. Ongoing shortening uplifted the foreland sediments [4] and the graphite was recycled once more in the modern fluvial network [5].

We propose that graphite-bearing rocks were eroded in China and deposited as poorly-lithified sediment in the South China Sea, the first cycle of erosion and burial. This sediment was exhumed as Taiwan emerged from the East China Sea (Chen et al., 2019). Since it had never been buried deeply, it was easily eroded and redeposited in the Pliocene and Pleistocene-age units of the Western Foothills (SED), which were the first to be sourced exclusively from terrestrial Taiwan (Chen et al., 2001). This is the second cycle of graphite transport. The continuing uplift and erosion of Taiwan has led to a third recycling event for the Highly Graphitized OC_{petro} particles, which have now been eroded from the western mountain front, via the Gaoping River, to the Gaoping Submarine Canyon (CN, SH) and onwards towards the Manila Trench (Fig. 5).

5.6. Impacts on the carbon cycle

Our study infers that the Highly graphitized OC_{petro} present in the Gaoping Canyon and Shelf off southwest Taiwan has survived at least three cycles of erosion, burial and exhumation. Hence, it is remarkably resilient, resisting oxidation or degradation during repeated exposure to oxygenated conditions, potentially accompanied by disruptive erosional processes, and also the effects of tectonic deformation, fluid-rock interaction, and microbial activity. Whereas more labile OC_{petro} can degrade or be lost during weathering, erosion and transport (Bouchez et al., 2010; Galy et al., 2007; Hilton et al., 2014), graphitization is clearly able to stabilize carbon for millions of years, even in settings with active tectonic shortening. When considering the carbon cycle in the context of mountain building, the likelihood of eroded fossil carbon being returned to the atmosphere by degradation to CO_2 depends on the degree of graphitization. Major orogenic events, causing moder-

ate to high-grade metamorphism, are likely stabilizing carbon as graphite. Alongside the weathering of silicate minerals with carbonic acid and biospheric OC burial, this mechanism adds to the role of mountain building in scrubbing CO_2 from the atmosphere.

Erosion in Taiwan delivers about 500 $Mt\,y^{-1}$ of sediment to the ocean (Dadson et al., 2003). Bedrock and river bedload samples from across Taiwan contain mean OC_{petro} concentrations of 0.24 and 0.27 wt% respectively (Hilton et al., 2010). Therefore, approximately 1 $Mt\,y^{-1}$ of OC_{petro} is delivered from the island, a similar amount to the combined OC_{petro} discharge of the Beni and Madre de Dios Rivers in the Andes (Clark et al., 2017). This is equivalent to an area-normalized OC_{petro} yield from Taiwan of approximately 30 $t\,km^{-2}\,y^{-1}$, twice the that of the Andean rivers (Clark et al., 2017). The graphitic proportion of this OC_{petro} is likely to be stable over long distances and geological timescales. The Grass Lake Creek sediments suggest that lower grade OC_{petro} is likely to survive transport and reburial over short distances, even if longer range transport leads to progressive loss of the more disordered material (Bouchez et al., 2010; Clark et al., 2017; Galy et al., 2008). Therefore, OC_{petro} oxidation in other erosive locations around the world should be a slow process compared to degradation of biosphere-derived OC. In the Arctic Ocean, OC_{petro} erosion from permafrost was tracked from the coastline across 500 km of continental shelf (Sparkes et al., 2018). The Taiwanese case suggests that the OC_{petro} component of the shelf deposits should survive on the shelf for thousands to millions of years, even if more labile biospheric OC is prone to degradation (Benner et al., 1997; Bröder et al., 2016; Hedges et al., 1997; Prahl et al., 1994; Salvadó et al., 2017; Sparkes et al., 2016). When calculating the likelihood of OC remineralization in erosive systems, care must be taken to differentiate material based on lability and not to treat the entire OC pool as equally vulnerable to degradation.

Finally, this study suggests that graphite flakes, being resistant to physical, chemical and biological degradation, can be used as geochemical tracers through extreme tectonic events, in a similar manner to e.g. zircons. Coupled with the relative ease of Raman measurements, this would suggest that in many situations graphite and other OC_{petro} can be excellent targets for studying erosional histories and tectonic events as a complement to traditional techniques.

6. Conclusions

By analyzing Raman spectra from multiple catchments within a complex tectonic system, we have shown that graphitic carbon can survive multiple orogenic cycles, being transported as microscopic flakes within the sediment load. Young sedimentary rocks in the Western Foothills of Taiwan contain highly crystalline graphite that must have experienced at least two erosional cycles. Sediments collected from the Gaoping River and Canyon suggest that these formations have supplied graphite to the submarine canyon, indicating a third cycle of erosion. Despite multiple sediment recycling events precluding permanent burial, graphitization of organic matter during orogenesis has led to a stabilization and sequestration of carbon over geological timescales.

7. Acknowledgements

RBS was supported by an Engineering and Physical Sciences Research Council studentship, grant numbers EP/P502365/1 and EP/P504120/1. JTL was supported by grant number NSC 95-2745-M-110-001 (National Science Council) for the Fate of Terrestrial-Nonterrestrial Sediments in High Yield Particle-Export River-Sea Systems Program, which provided the cores in this study. Robert Emberson provided the Chenyoulan River samples. A. Joshua West assisted with the Laonung River fieldwork. Olivier Beyssac provided training in Raman spectroscopy. We thank the editor and one anonymous reviewer for their helpful comments.

8. List of supporting information

- Supplementary Method Details: calculations of the proportion of each lithology in each catchment; an extended description of the Raman spectra collection and analysis procedure; a description of the sample collection details, including location, grainsize and sample type
- Raman data: Table including metadata from the peak fitting procedure described in the manuscript and supplementary methods file. The peak locations, heights, widths and areas for each identified peak are reported, along with height and area ratios.

Declaration of competing interest

The authors declare that they have no known competing financial interests or personal relationships that could have appeared to influence the work reported in this paper.

Appendix A. Supplementary material

Supplementary material related to this article can be found online at https://doi.org/10.1016/j.epsl.2019.115992.

References

Benner, R., Biddanda, B., Black, B., McCarthy, M., 1997. Abundance, size distribution, and stable carbon and nitrogen isotopic compositions of marine organic matter isolated by tangential-flow ultrafiltration. Mar. Chem. 57, 243–263. https://doi.org/10.1016/S0304-4203(97)00013-3.

Beyssac, O., Goffe, B., Chopin, C., Rouzaud, J., 2002a. Raman spectra of carbonaceous material in metasediments: a new geothermometer. J. Metamorph. Geol. 20, 859–871. https://doi.org/10.1046/j.1525-1314.2002.00408.x.

Beyssac, O., Rouzaud, J., Goffe, B., Brunet, F., Chopin, C., 2002b. Graphitization in a high-pressure, low-temperature metamorphic gradient: a Raman microspectroscopy and HRTEM study. Contrib. Mineral. Petrol. 143, 19–31. https://doi.org/10.1007/s00410-001-0324-7.

Beyssac, O., Brunet, F., Petitet, J.P., Bruno Goffe, B., Rouzaud, J.N., 2003. Experimental study of the microtextural and structural transformations of carbonaceous materials under pressure and temperature. Eur. J. Mineral. 15, 937–951.

Beyssac, O., Simoes, M., Avouac, J., Farley, K., Chen, Yue-Gau, Chan, Yu-Chang, 2007, Goffe, B. Late Cenozoic metamorphic evolution and exhumation of Taiwan. Tectonics 26, TC6001. https://doi.org/10.1029/2006TC002064.

Bouchez, J., Beyssac, O., Galy, V., Gaillardet, J., France-Lanord, C., Maurice, L., Moreira-Turcq, P., 2010. Oxidation of petrogenic organic carbon in the Amazon floodplain as a source of atmospheric CO(2). Geology 38, 255–258. https://doi.org/10.1130/G30608.1.

Bröder, L., Tesi, T., Andersson, A., Eglinton, T.I., Semiletov, I.P., Dudarev, O.V., Roos, P., Gustafsson, Ö., 2016. Historical records of organic matter supply and degradation status in the East Siberian Sea. Org. Geochem. 91, 16–30. https://doi.org/10.1016/j.orggeochem.2015.10.008.

Carter, L., Gavey, R., Talling, P.J., Liu, J.T., 2014. Insights into submarine geohazards from breaks in subsea telecommunication cables. Oceanography 27. https://doi.org/10.5670/oceanog.2014.40.

Chen, C., Chu, H., Liou, J., Ernst, W., 1983. Explanatory notes for the metamorphic facies map of Taiwan. Spec. Pub. Centr. Geol. Surv. 2, 1–32.

Chen, C.H., Ho, H.C., Shea, K.S., Lo, W., Lin, W.H., Chang, H.C., Huang, C.S., Lin, C.W., Chen, G.H., Yang, C.N., Lee, Y.H., 2000. Geologic Map of Taiwan. Technical Report. Central Geological Survey, Ministry of Economic Affairs, Taiwan.

Chen, W., Ridgway, K., Horng, C., Chen, Y., Shea, K., Yeh, M., 2001. Stratigraphic architecture, magnetostratigraphy, and incised-valley systems of the Pliocene-Pleistocene collisional marine foreland basin of Taiwan. Geol. Soc. Am. Bull. 113, 1249–1271.

Chen, W.S., Yeh, J.J., Syu, S.J., 2019. Late Cenozoic exhumation and erosion of the Taiwan orogenic belt: new insights from petrographic analysis of foreland basin sediments and thermochronological dating on the metamorphic orogenic wedge. Tectonophysics 750, 56–69. https://doi.org/10.1016/j.tecto.2018.09.003.

Clark, K.E., Hilton, R.G., West, A.J., Robles Caceres, A., Gröcke, D.R., Marthews, T.R., Ferguson, R.I., Asner, G.P., New, M., Malhi, Y., 2017. Erosion of organic carbon from the Andes and its effects on ecosystem carbon dioxide balance. J. Geophys. Res., Biogeosci. 122, 449–469. https://doi.org/10.1002/2016JG003615.

Dadson, S., Hovius, N., Chen, H., Dade, W., Hsieh, M., Willett, S., Hu, J., Horng, M., Chen, M., Stark, C., Lague, D., Lin, J., 2003. Links between erosion, runoff variability and seismicity in the Taiwan orogen. Nature 426, 648–651. https://doi.org/10.1038/nature02150.

France-Lanord, C., Derry, L.A., 1997. Organic carbon burial forcing of the carbon cycle from Himalayan erosion. Nature 390, 65–67. https://doi.org/10.1038/36324.

Galy, V., France-Lanord, C., Beyssac, O., Faure, P., Kudrass, H., Palhol, F., 2007. Efficient organic carbon burial in the bengal fan sustained by the Himalayan erosional system. Nature 450, 407–410. https://doi.org/10.1038/nature06273.

Galy, V., Beyssac, O., France-Lanord, C., Eglinton, T., 2008. Recycling of graphite during Himalayan erosion: a geological stabilization of carbon in the crust. Science 322, 943–945. https://doi.org/10.1126/science.1161408.

Hedges, J.I., Keil, R.G., Benner, R., 1997. What happens to terrestrial organic matter in the ocean? Org. Geochem. 27, 195–212. https://doi.org/10.1016/j.marchem.2004.06.033.

Hemingway, J.D., Hilton, R.G., Hovius, N., Eglinton, T.I., Haghipour, N., Wacker, L., Chen, M.C., Galy, V.V., 2018. Microbial oxidation of lithospheric organic carbon in rapidly eroding tropical mountain soils. Science 360, 209–212. https://doi.org/10.1126/science.aao6463.

Hilton, R.G., Galy, A., Hovius, N., Chen, M.C., Horng, M.J., Chen, H., 2008. Tropical-cyclone-driven erosion of the terrestrial biosphere from mountains. Nat. Geosci. 1, 759–762. https://doi.org/10.1038/ngeo333.

Hilton, R.G., Galy, A., Hovius, N., Horng, M.J., Chen, H., 2010. The isotopic composition of particulate organic carbon in mountain rivers of Taiwan. Geochim. Cosmochim. Acta 74, 3164–3181. https://doi.org/10.1016/j.gca.2010.03.004.

Hilton, R.G., Gaillardet, J., Calmels, D., Birck, J.L., 2014. Geological respiration of a mountain belt revealed by the trace element rhenium. Earth Planet. Sci. Lett. 403, 27–36. https://doi.org/10.1016/j.epsl.2014.06.021.

Hilton, R.G., Galy, V., Gaillardet, J., Dellinger, M., Bryant, C., O'Regan, M., Grocke, D.R., Coxall, H., Bouchez, J., Calmels, D., 2015. Erosion of organic carbon in the Arctic as a geological carbon dioxide sink. Nature 524, 84–87. https://doi.org/10.1038/nature14653.

Kao, S.J., Hilton, R.G., Selvaraj, K., Dai, M., Zehetner, F., Huang, J.C., Hsu, S.C., Sparkes, R., Liu, J.T., Lee, T.Y., Yang, J.Y.T., Galy, A., Xu, X., Hovius, N., 2014. Preservation of terrestrial organic carbon in marine sediments offshore Taiwan: mountain building and atmospheric carbon dioxide sequestration. Earth Surf. Dyn. 2, 127–139. https://doi.org/10.5194/esurf-2-127-2014.

Lahfid, A., Beyssac, O., Deville, E., Negro, F., Chopin, C., Goffe, B., 2010. Evolution of the Raman spectrum of carbonaceous material in low-grade metasediments of the Glarus Alps (Switzerland). Terra Nova 22, 354–360. https://doi.org/10.1111/j.1365-3121.2010.00956.x.

Liu, J.T., Wang, Y.H., Yang, R.J., Hsu, R.T., Kao, S.J., Lin, H.L., Kuo, F.H., 2012. Cyclone-induced hyperpycnal turbidity currents in a submarine canyon. J. Geophys. Res. https://doi.org/10.1029/2011JC007630.

Liu, J.T., Kao, S.J., Huh, C.A., Hung, C.C., 2013. Gravity flows associated with flood events and carbon burial: Taiwan as instructional source area. Annu. Rev. Mar. Sci. 5, 47–68. https://doi.org/10.1146/annurev-marine-121211-172307.

Liu, J.T., Hsu, R.T., Hung, J.J., Chang, Y.P., Wang, Y.H., Rendle-Bühring, R.H., Lee, C.L., Huh, C.A., Yang, R.J., 2016. From the highest to the deepest: the gaoping river-gaoping submarine canyon dispersal system. Earth-Sci. Rev. 153, 274–300. https://doi.org/10.1016/j.earscirev.2015.10.012.

Nibourel, L., Herman, F., Cox, S.C., Beyssac, O., Lav'e, J., 2015. Provenance analysis using Raman spectroscopy of carbonaceous material: a case study in the southern Alps of New Zealand. J. Geophys. Res., Earth Surf. 120, 2056–2079. https://doi.org/10.1002/2015JF003541. 2015JF003541.

Petsch, S.T., Berner, R.A., Eglinton, T.I., 2000. A field study of the chemical weathering of ancient sedimentary organic matter. Org. Geochem. 31, 475–487. https://doi.org/10.1016/S0146-6380(00)00014-0.

Prahl, F., Ertel, J., Goni, M., Sparrow, M., Eversmeyer, B., 1994. Terrestrial organic carbon contributions to sediments on the Washington margin. Geochim. Cosmochim. Acta 58, 3035–3048. https://doi.org/10.1016/0016-7037(94)90177-5.

Salvadó, J.A., Bröder, L., Andersson, A., Semiletov, I.P., Gustafsson, O., 2017. Release of black carbon from thawing permafrost estimated by sequestration fluxes in the East Siberian Arctic shelf recipient. Glob. Biogeochem. Cycles 31, 1501–1515. https://doi.org/10.1002/2017GB005693. 2017GB005693.

Scheingross, J.S., Hovius, N., Dellinger, M., Hilton, R., Repasch, M., Sachse, D., Gröcke, D., Vieth-Hillebrand, A., Turowski, J., 2019. Preservation of organic carbon during active fluvial transport and particle abrasion. Geology. https://doi.org/10.1130/G46442.1.

Sparkes, R., Hovius, N., Galy, A., Kumar, R.V., Liu, J.T., 2013. Automated analysis of carbon in powdered geological and environmental samples by Raman spectroscopy. Appl. Spectrosc. 67, 779–788. https://doi.org/10.1366/12-06826.

Sparkes, R.B., Lin, I.T., Hovius, N., Galy, A., Liu, J.T., Xu, X., Yang, R., 2015. Redistribution of multi-phase particulate organic carbon in a marine shelf and canyon system during an exceptional river flood: effects of typhoon morakot on the gaoping river-canyon system. Mar. Geol. 363, 191–201. https://doi.org/10.1016/j.margeo.2015.02.013.

Sparkes, R.B., Doğrul Selver, A., Gustafsson, O., Semiletov, I.P., Haghipour, N., Wacker, L., Eglinton, T.I., Talbot, H.M., van Dongen, B.E., 2016. Macromolecular composition of terrestrial and marine organic matter in sediments across the East Siberian Arctic shelf. Cryosphere 10, 2485–2500. https://doi.org/10.5194/tc-10-2485-2016.

Sparkes, R.B., Maher, M., Blewett, J., Doğrul Selver, A., Gustafsson, O., Semiletov, I.P., van Dongen, B.E., 2018. Carbonaceous material export from Siberian permafrost tracked across the Arctic shelf using Raman spectroscopy. Cryosphere 12, 3293–3309. https://doi.org/10.5194/tc-12-3293-2018.

Teng, L., 1990. Geotectonic evolution of late Cenozoic arc continent collision in Taiwan. Tectonophysics 183, 57–76. https://doi.org/10.1016/0040-1951(90)90188-E.

Walsh, J.J., Rowe, G.T., Iverson, R.L., McRoy, C.P., 1981. Biological export of shelf carbon is a sink of the global CO2 cycle. Nature 291, 196–201. https://doi.org/10.1038/291196a0.

Wilde, S.A., Dorsett-Bain, H.L., Lennon, R.G., 1999. Geological setting and controls on the development of graphite, sillimanite and phosphate mineralization within the Jiamusi Massif: an exotic fragment of Gondwanaland located in North-eastern China? Gondwana Res. 2, 21–46. https://doi.org/10.1016/S1342-937X(05)70125-8.

Ye, Q., Tong, J., Tian, L., Hu, J., An, Z., Bodnar, R.J., Xiao, S., 2019. Detrital graphite particles in the cryogenian nantuo formation of South China: implications for sedimentary provenance and tectonic history. Precambrian Res. 323, 6–15. https://doi.org/10.1016/j.precamres.2019.01.003.

Yui, T.F., Chu, H.T., 2000. 'Overturned' marble layers: evidence for upward extrusion of the backbone range of Taiwan. Earth Planet. Sci. Lett. 179, 351–361. https://doi.org/10.1016/S0012-821X(00)00119-9.

Zheng, H., Clift, P.D., Wang, P., Tada, R., Jia, J., He, M., Jourdan, F., 2013. Pre-miocene birth of the Yangtze River. Proc. Natl. Acad. Sci. 110, 7556–7561. https://doi.org/10.1073/pnas.1216241110.

Zheng, Z., Zhang, J., Huang, J., 1996. Observations of microstructure and reflectivity of coal graphites for two locations in China. Int. J. Coal Geol. 30, 277–284. https://doi.org/10.1016/0166-5162(95)00047-X. coalification and Coal Petrology.